Molecular Therapy
Nucleic Acids
Original Article

Depleting hepatitis B virus relaxed circular DNA is necessary for resolution of infection by CRISPR-Cas9

Dmitry Kostyushev,[1,2,15,16] Anastasiya Kostyusheva,[1,16] Sergey Brezgin,[1,2,16] Natalia Ponomareva,[1,2,3] Natalia F. Zakirova,[4] Aleksandra Egorshina,[1] Dmitry V. Yanvarev,[4] Ekaterina Bayurova,[5] Anna Sudina,[6] Irina Goptar,[7] Anastasiya Nikiforova,[7] Elena Dunaeva,[8] Tatiana Lisitsa,[6] Ivan Abramov,[6] Anastasiia Frolova,[9] Alexander Lukashev,[1] Ilya Gordeychuk,[5,10] Andrey A. Zamyatnin, Jr.,[2,9,11,12] Alexander Ivanov,[4] and Vladimir Chulanov[2,10,13,14,15]

[1]Martsinovsky Institute of Medical Parasitology, Tropical and Vector-Borne Diseases, Sechenov University, Moscow 119991, Russia; [2]Scientific Center for Genetics and Life Sciences, Division of Biotechnology, Sirius University of Science and Technology, Sochi 354340, Russia; [3]Department of Pharmaceutical and Toxicological Chemistry, Sechenov First Moscow State Medical University, Moscow 119146, Russia; [4]Center for Precision Genome Editing and Genetic Technologies for Biomedicine, Engelhardt Institute of Molecular Biology, Russian Academy of Science, Moscow 119991, Russia; [5]Chumakov Federal Scientific Center for Research and Development of Immune-and-Biological Products of Russian Academy of Sciences, Moscow 108819, Russia; [6]Federal State Budgetary Institution Centre for Strategic Planning and Management of Biomedical Health Risks of the Federal Medical Biological Agency, Moscow 119435, Russia; [7]Izmerov Research Institute of Occupational Health, Moscow 105275, Russia; [8]Central Research Institute of Epidemiology, Moscow 111123, Russia; [9]Institute of Molecular Medicine, Sechenov First Moscow State Medical University, Moscow 119991, Russia; [10]Institute for Translational Medicine and Biotechnology, Sechenov First Moscow State Medical University, Moscow 127994, Russia; [11]Belozersky Institute of Physico-Chemical Biology, Lomonosov Moscow State University, Moscow 119992, Russia; [12]Faculty of Health and Medical Sciences, University of Surrey, Guildford GU2 7XH, UK; [13]Department of Infectious Diseases, Sechenov First Moscow State Medical University, Moscow 119146, Russia; [14]National Medical Research Center of Tuberculosis and Infectious Diseases, Ministry of Health, Moscow 127994, Russia

CRISPR-Cas9 systems can directly target the hepatitis B virus (HBV) major genomic form, covalently closed circular DNA (cccDNA), for decay and demonstrate remarkable anti-HBV activity. Here, we demonstrate that CRISPR-Cas9-mediated inactivation of HBV cccDNA, frequently regarded as the "holy grail" of viral persistence, is not sufficient for curing infection. Instead, HBV replication rapidly rebounds because of *de novo* formation of HBV cccDNA from its precursor, HBV relaxed circular DNA (rcDNA). However, depleting HBV rcDNA before CRISPR-Cas9 ribonucleoprotein (RNP) delivery prevents viral rebound and promotes resolution of HBV infection. These findings provide the groundwork for developing approaches for a virological cure of HBV infection by a single dose of short-lived CRISPR-Cas9 RNPs. Blocking cccDNA replenishment and re-establishment from rcDNA conversion is critical for completely clearing the virus from infected cells by site-specific nucleases. The latter can be achieved by widely used reverse transcriptase inhibitors.

INTRODUCTION

Hepatitis B virus (HBV) is a highly contagious virus known to infect humans and cause chronic hepatitis B (CHB).[1] CHB is a leading cause of liver cancer and cirrhosis worldwide, with approximately 1 million deaths annually.[2] Modern therapeutics suppress viral replication but cannot clear viral infection and thus do not induce durable post-treatment control of viral replication in a significant portion of CHB patients.[3] HBV's covalently closed circular DNA (cccDNA), residing in the nuclei of infected hepatocytes, is believed to be the source of viral persistence, causing rebound of viral replication after cessation of treatment.[4] Destroying HBV cccDNA in infected cells is thought to lead to the virological cure of HBV infection and complete eradication of the virus from the body.[5]

To date, the only molecular tools able to directly target HBV cccDNA are site-specific nucleases, including CRISPR-Cas9.[6] CRISPR-Cas9 has been reported to efficiently and precisely cleave HBV cccDNA, leading to dramatic decline in viral levels.[7–13] However, recent findings suggest that HBV replication could also be maintained by re-infection with circulating HBV particles and nuclear re-import of relaxed circular DNA (rcDNA), the precursor of HBV cccDNA.[14] We therefore asked how a single delivery of highly effective CRISPR-Cas9 ribonucleoproteins (RNPs) could affect HBV replication, and whether conversion of rcDNA into cccDNA can result in re-establishing viral replication after HBV cccDNA degradation.

Received 10 August 2022; accepted 1 February 2023;
https://doi.org/10.1016/j.omtn.2023.02.001.

[15]Senior author

[16]These authors contributed equally

Correspondence: Dmitry Kostyushev, Martsinovsky Institute of Medical Parasitology, Tropical and Vector-Borne Diseases, Sechenov University, Malaya Pirogovskaya 20 st., bld. 1, office 207, Moscow 119991, Russia.
E-mail: dkostushev@gmail.com

Although many studies employed CRISPR-Cas for targeting HBV cccDNA,[7–9,12,13,15–17] they mostly relied on prolonged intracellular overexpression of CRISPR-Cas from plasmid vectors and thus could not estimate their antiviral activity in a clinically relevant setting. Several studies also demonstrated that reverse transcriptase inhibitors, including lamivudine, tenofovir disoproxil fumarate, and entecavir, provide a cumulative improvement when used together with CRISPR-Cas.[11,18] However, the rebound of HBV replication after CRISPR-Cas delivery has never been directly assessed. In this study, for the first time we demonstrate the rebound of HBV replication following highly effective CRISPR-Cas9-mediated suppression of viral replication and develop a simple strategy to prevent viral reactivation by depleting the HBV rcDNA genomic form using reverse transcriptase inhibitors.

Here, we report that: (1) a single, transient delivery of CRISPR-Cas9 RNPs eradicates >98% of HBV cccDNA; (2) the cccDNA pool is re-established, and HBV replication rebounds after CRISPR-Cas9 RNP degradation; and (3) depleting HBV rcDNA in infected cells with lamivudine, a reverse transcriptase inhibitor, prevents re-establishment of cccDNA and promotes resolution of HBV infection by a single dose of CRISPR-Cas9 RNPs. Besides this, we demonstrate that epigenetic modification (DNA methylation) of cccDNA hampers or blocks cccDNA cleavage by *Streptococcus thermophilus* CRISPR-Cas9 (StCas9), although this effect can be overcome by increasing doses of CRISPR-Cas9 RNPs. Overall, in this study we provide the groundwork for developing approaches aimed at curing HBV infection.

RESULTS

Robust anti-HBV activity of a single dose of CRISPR-Cas9 RNPs

CRISPR-Cas9 RNPs rapidly edit target DNA shortly after delivery.[19] Less than 24 h post delivery, RNPs are largely destroyed by endogenous nucleases and proteases and no longer function. The limited lifetime and burst-like kinetics of RNPs result in very efficient on-target activity and markedly reduced off-target mutagenesis.[19] To test on-target nucleolytic activity, we assembled RNPs of StCas9 with one of the *in vitro*-transcribed, HBV-specific single guide RNAs (sgRNAs) (St3, St4, or St10) (Figure 1A)[13] and performed a biochemical *in vitro* cleavage assay with recombinant cccDNA (rcccDNA). Using any of the three sgRNAs, StCas9 effectively cleaved HBV rcccDNA, as evidenced by generation of a single band on gel electrophoresis corresponding to linear rcccDNA (Figure 1B). When transfected into HepG2 cells with HBV rcccDNA (Figure 1C), RNPs led to reduced HBV viral transcription (pregenomic RNA [pgRNA] and S-mRNA levels) and replication (marked decrease in HBV DNA and rcccDNA levels) (Figure 1D). St3 sgRNA was the least effective, leading to ~50% rcccDNA reduction, while St10 displayed the highest antiviral activity with over 98% drop in rcccDNA levels. Successful intranuclear delivery of StCas9 was validated by immunocytochemistry 20 h post transfection (Figure 1E). Nucleofected StCas9 decayed and was not detected at 24 h post transfection (Figure S1). Next, we used StCas9/St10 RNPs and measured anti-HBV activity at the protein level (Figures 1F–1H). Both hepatitis B core antigen (HBcAg) and surface antigen (HBsAg) were strongly reduced by StCas9/St10 RNPs (Figures 1G and 1H).

HBV rcccDNA cleaved by CRISPR-Cas9 is either repaired by non-homologous end-joining (NHEJ) or alternative pathways with the formation of disruptive or non-disruptive mutations,[7] or is degraded.[12,13,20] NHEJ inhibitor NU7026 hinders HBV rcccDNA degradation and may be used to assess the rates of rcccDNA degradation.[12] To determine the outcomes of HBV rcccDNA cleavage after CRISPR-Cas9 RNP treatment, we performed experiments with and without NU7026 and analyzed indels at different time points (Figure 1I). HBV rcccDNA was reduced >90% in HepG2 cells transfected with StCas9/St10 RNPs and treated with DMSO only, followed by a steady increase in HBV rcccDNA by day 4 post transfection (Figure 1J). Treating RNP-transfected cells with NU7026 significantly attenuated HBV rcccDNA decline at day 1 post transfection, which is consistent with our previous observations that NU7026 prevents degradation of HBV cccDNA.[12] Next, we deep-sequenced target HBV rcccDNA at days 1–4 post transfection and found different kinetics of HBV rcccDNA repair in normal and altered (treated with NU7026) conditions (Figure 1K). The majority of HBV rcccDNA was rapidly destroyed as evidenced by PCR (Figure 1J). The remaining HBV rcccDNAs were extensively edited with the formation of deletions of different size using StCas9 RNPs 3 days post transfection, indicating the slow repair kinetics of Cas9-induced double-strand breaks (DSBs).[21] Insertions were absent or extremely rare, and deletions were absent the following day. In contrast, high rates of deletions were detected as early as 2 days post transfection at the site of nucleolytic cleavage when NU7026 was used, followed by a switch to frequent on-target insertions at day 3 post transfection. Indels were not detected in the St10 + NU7026 group 4 days post transfection. This is consistent with the effects of NHEJ inhibitors on DSB repair kinetics, which alter the outcome of DNA cleavage and result in more rapid repair of DSBs by alternative pathways.[21,22]

Disappearance of mutations in HBV rcccDNA at later time points and markedly reduced HBV cccDNA levels indicate that the majority of HBV rcccDNA cleaved by RNPs may be destroyed. When using NU7026, rcccDNA declined less abruptly but harbored frequent and heterogeneous indels (Figures S2A and S2B).

As off-target mutagenesis inflicted by CRISPR-Cas9 is a major concern that may compromise its potential clinical application and may compromise cell function, we deep-sequenced an array of 12 off-target host genome sites with the highest probability of cleavage. No significant increase in mutations was detected at any of these sites compared with control RNPs. The indel frequency at all loci ranged from 0% to 0.1%. Indel distribution analysis revealed background indels that did not form a pattern typical for CRISPR-Cas9-induced mutagenesis (Figure S3). These results show that the designed RNPs exclusively target HBV DNA and do not affect the host genome.

Prevention of HBV rcccDNA cleavage by methylation

Methylation of cccDNA is a host defense mechanism aimed at transcriptionally silencing the virus. Three canonical and several

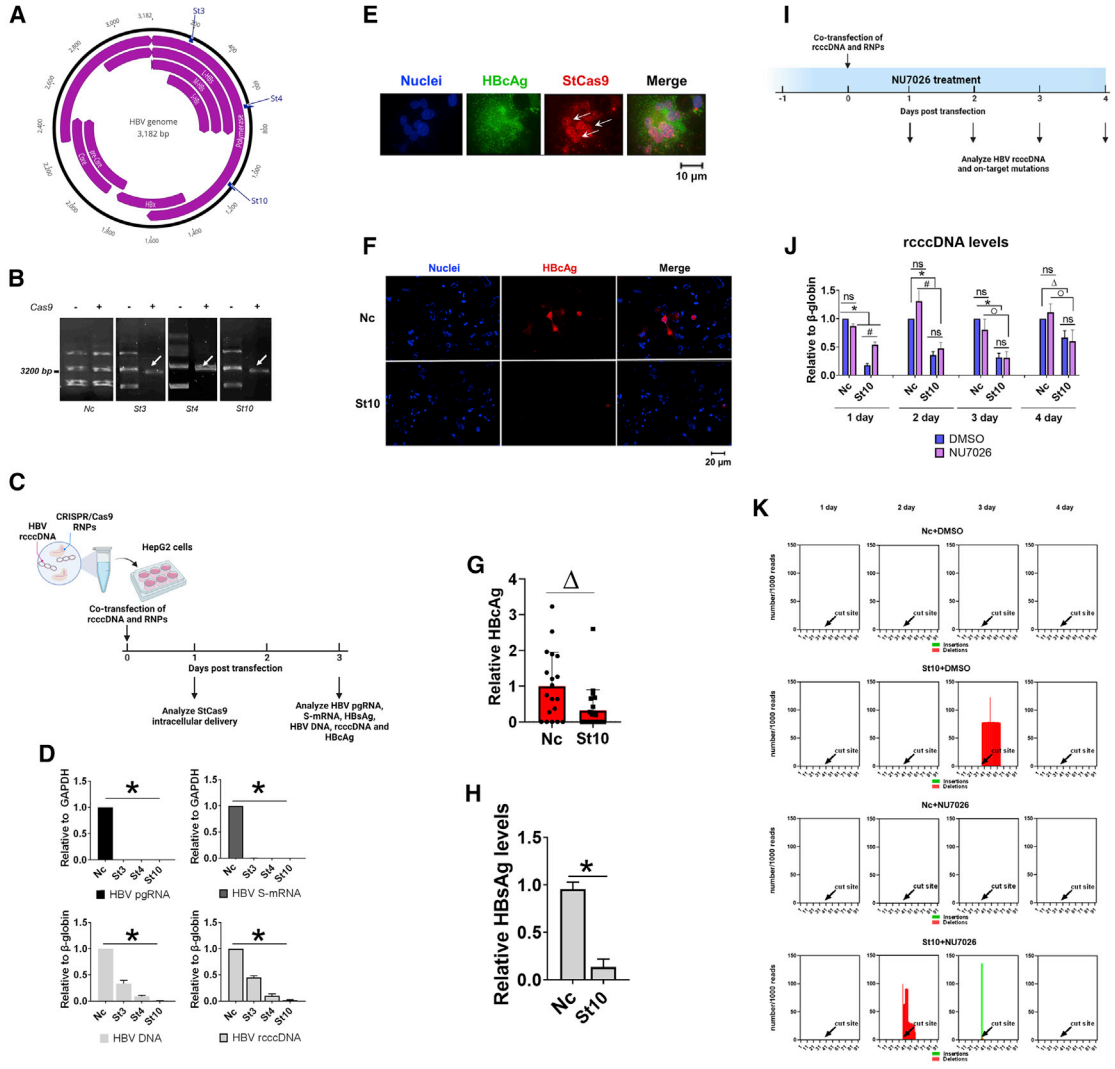

Figure 1. Potent anti-HBV activity of CRISPR-Cas9 RNPs

(A) Targets of CRISPR-Cas9 in the HBV genome. (B) *In vitro* digestion assay of HBV rcccDNA by CRISPR-Cas9. Arrows indicate digested rcccDNA, seen as a single band on gel electrophoresis. (C) Experimental setup of CRISPR-Cas9 RNPs transfection. (D) Anti-HBV activity of CRISPR-Cas9 analyzed by measuring pgRNA and HBV S-mRNA normalized to GAPDH mRNA, and by measuring HBV DNA and rcccDNA relative to β-globin. (E) Intracellular delivery of StCas9 protein. HBcAg (green) and StCas9 protein (red); cell nuclei were labeled by Hoechst 33342 dye (blue). (F) Analysis of HBcAg expression, (G and H) Relative levels of (G) HBcAg-positive cells and (H) HBsAg secretion. (I) NU7026 experimental setup. (J) PCR analysis of HBV cccDNA levels with and without NU7026 treatment (relative to β-globin). (K) Indel rates in cccDNA. All groups were transfected with rcccDNA and either StCas9 protein with non-targeting sgRNA (Nc) or HBV-specific St10 (St10) sgRNA, and treated with DMSO (+DMSO) or NU7026 (+NU7026). $^{\circ}p < 0.05$, $^{\Delta}p < 0.01$, $^{\#}p < 0.001$, $^{*}p < 0.0001$; ns, not significant. (C) and (I) were created in BioRender.

non-canonical CpG islands and non-CpG sites in the HBV genome are subjected to DNA methylation (Figure 2A). Different HBV genotypes contain distinct CpG islands and are unequally methylated.[23] The extent of HBV cccDNA methylation correlates with CHB progression.[23] DNA methylation is a layer of patient-to-patient and inter-genotype variation[23] that may change upon disease progression and treatment[24,25] and, potentially, compromise nucleolytic activity of CRISPR-Cas9 systems.[26,27] To unravel the effects of HBV rcccDNA methylation on RNP activity, we generated heavily methylated rcccDNA (meth-rcccDNA) (Figure 2B) as described previously.[13] *In vitro* cleavage assay demonstrated that rcccDNA methylation drastically reduced StCas9 cleavage with St3 sgRNA (~91% of rcccDNA versus ~47% of meth-rcccDNA) and with St10 sgRNA (~86% of rcccDNA versus ~16% of meth-rcccDNA) (Figure 2C), the target sites of which are located in CpG I and CpG II islands (Figure 2A), respectively. Activity of StCas9 with St4 sgRNA, which targets a site outside CpG islands, was unaltered (Figure 2C). To further characterize the effect of rcccDNA methylation on StCas9 RNP activity,

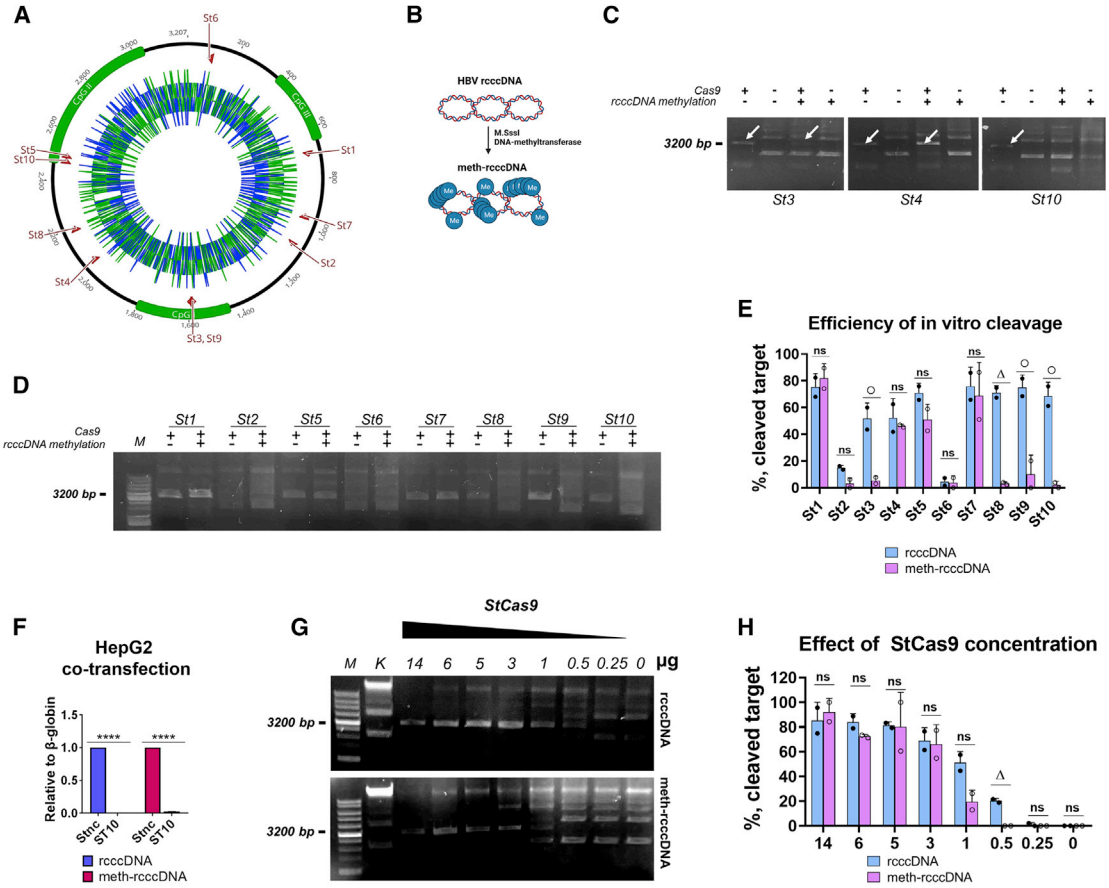

Figure 2. Effects of HBV rcccDNA methylation on target digestion and antiviral activity by CRISPR-Cas9 RNPs

(A) Distribution of CpG islands (I–III) and graphs showing GC content (blue line) and AT content (green line) (a sliding window of 4 nucleotides). St1–St10 sgRNA targets are shown on the HBV genome map. (B) Schematic depicting HBV rcccDNA methylation by M.SssI DNA methyltransferase. Me, methylated cytosines. (C and D) *In vitro* digestion reaction of rcccDNA and meth-rcccDNA by StCas9 RNPs. Arrows indicate digested rcccDNA. (E) Relative levels of rcccDNA/meth-rcccDNA digestion by StCas9 RNPs. (F) PCR analysis of rcccDNA and meth-rcccDNA levels (relative to β-globin) after transfection of StCas9/St10 RNPs (St10) or mock treatment (Nc). (G and H) (G) Effect of dose on the ability of StCas9/St10 RNPs to cleave meth-rcccDNA and (H) its semi-quantitative evaluation. M, marker; K, mock-treated control. $^{\circ}p < 0.05$, $^{\Delta}p < 0.01$, $^{\#}p < 0.001$, $^{*}p < 0.0001$; ns, not significant. (B) was created in BioRender.

we assembled StCas9 RNPs with every sgRNA able to target HBV rcccDNA (Figure 2A)[13] and performed *in vitro* cleavage reactions (Figures 2D and 2E). Out of ten StCas9 sgRNAs, eight sgRNAs cleaved rcccDNA with >50% efficiency (Figure 2E); St2 and St6 cleaved less than 20% of rcccDNA and were further not taken into analysis. In addition to St3 and St10, rcccDNA cleavage with sgRNAs St8 and St9 was strongly affected by DNA methylation (Figures 2D and 2E). Along with St4, activity of sgRNAs St1, St5, and St7 was unaltered at methylated rcccDNA. Surprisingly, analysis of sgRNA target sequences revealed that target site nucleotide composition and CpG content were not important for RNP cleavage of methylated rcccDNA (Figures S4A–S4E), although there was a preponderance for sgRNAs targeting regions outside of CpG islands to cut rcccDNA irrespective of DNA methylation (Figures S4A and S4B). Targets of sgRNAs inside CpG islands were mostly affected by methylation (Figures S4A and S4B). The lack of strong reliance of DNA methylation effects on the target nucleotide sequence may arise from different efficiency of rcccDNA methylation at certain positions. Indeed, HBV rcccDNA synthesized *in vitro* was heavily methylated as evidenced by bisulfite sequencing, but the rates of methylation differed from 65% to 91% (Figure S5).

Next, we analyzed the effects of rcccDNA methylation on StCas9 RNP activity in HepG2 cells. Transfection of StCas9/St10 RNPs with meth-rcccDNA into HepG2 cells reduced rcccDNA levels similarly to using unmethylated rcccDNA (Figure 2F). This indicated that intracellularly, DNA methylation does not affect nucleolytic cleavage. Bisulfite sequencing confirmed that rcccDNA stays heavily methylated up to 3 days post transfection (methylation of cytosines ranged from 21%–52% to 65%–100% at different positions) (Figure S6). Hence, a potential role of rcccDNA demethylation may be ruled out. The difference between biochemical assays and cell-culture experiments

could be explained by the higher doses of RNPs used in HepG2 transfection in the biochemical assay. Thus, we performed *in vitro* biochemical cleavage assays with the same amounts of rcccDNA and meth-rcccDNA but with different amounts of StCas9 protein (within a range of 0.25–14 μg per reaction) (Figures 2G and 2H). At lower dosages (0.25 μg and 1 μg per reaction), rcccDNA methylation strongly reduced RNP activity, while increasing amounts of StCas9 protein overcame DNA methylation and effectively cleaved the target (Figures 2G and 2H). From these results, for the first time we demonstrate that HBV DNA methylation hinders rcccDNA cleavage by StCas9, although this effect is overcome by increasing RNP dosage.

Rebound of HBV replication and the effect of rcDNA depletion

To evaluate the effects of a single StCas9/St10 RNP administration on HBV replication, we observed HBV rcccDNA, intracellular HBV DNA, pgRNA, and secreted HBsAg and HBcAg levels for 14 days (Figures 3A and S7A). By the fourth day post transfection, all HBV parameters tested were still prominently (>90%) reduced (Figures 3B–3F and S7A); however, rcccDNA, intracellular HBV DNA, pgRNA, and secreted HBsAg and HBcAg levels gradually reached control levels by the 14th day. This indicates that HBV replication rebounds after almost complete eradication by StCas9/St10 RNPs. To determine whether HBV relapse requires rcccDNA to be transcriptionally active, we performed experiments with rcccDNA and transcriptionally silenced meth-rcccDNA, as shown in Figure 3A. As expected, rcccDNA levels recovered by the 17th day while meth-rcccDNA did not, remaining below 85%–98% of the control (Figure 3G). This suggested that HBV rebound is related either to the activity of uncut rcccDNA or to rcDNA produced from rcccDNA-transcribed pgRNA.

To study the role of rcDNA in HBV rebound, we pre-treated HepG2 cells with lamivudine (LAM), a reverse transcriptase inhibitor, 1 day before transfection and kept it in the culture medium for the next 6 days, replenishing the medium with fresh LAM every 2 days (Figure 3H). LAM prevents formation of rcDNA; rcDNA was almost absent in cells, and new cccDNA could not be formed from rcDNA. On day 5, LAM was removed from culture medium and HBV parameters were measured for the next 14 days (up to day 19 post transfection so that the observation periods in LAM and no-LAM experiments are identical) to evaluate the effect of rcDNA depletion on HBV rebound. HBV cccDNA, intracellular HBV DNA, pgRNA, and secreted HBsAg remained virtually at the same residual levels (Figures 3I–3L), and HBcAg was reduced, but not statistically significantly, compared with control (Figures 3M and S7B). Southern blotting confirmed rebound of HBV replication after transfection of RNPs and demonstrated a substantial reduction in HBV DNA upon rcDNA depletion by LAM (Figure 3N). Altogether, these results indicate that rebound of HBV replication after rcccDNA eradication by CRISPR-Cas9 RNPs can be prevented if the HBV rcDNA → cccDNA step is abrogated.

Resolution of HBV infection by CRISPR-Cas9 RNPs

Initially, we used a co-transfection model to ensure the highest rates of HBV rcccDNA and CRISPR-Cas9 RNPs co-delivery into difficult-to-transfect HepG2 cells. However, (1) this model does not support complete HBV replication cycle, (2) rcccDNA-driven replication declines in time due to cell division, and (3) rcccDNA is a mimic of cccDNA, as a "true" HBV cccDNA is established only in an infection system. In this respect, we nucleofected CRISPR-Cas9 RNPs into HBV-infected HepG2-hNTCP cells with or without LAM pre-treatment as shown in Figure 4A.

In this model, all analyzed HBV intermediates were remarkably reduced (∼95% for intracellular HBV DNA, ∼86% for HBV cccDNA, and ∼60% for secreted HBsAg) upon CRISPR-Cas9 RNP nucleofection with LAM pre-treatment (group St10 + LAM) by day 17 post nucleofection, whereas in a control group (Nc) HBV replication was amplified (Figures 4B–4D). Notably, in St10 + LAM group not only HBV levels did not amplify by day 17 post nucleofection but they consistently declined compared with day 7 post nucleofection.

The effect of CRISPR-Cas9 RNPs (St10) alone was not observed at day 7 post nucleofection. By the end of the observation HBV DNA, cccDNA, and HBsAg levels were all amplified but were significantly lower compared with the Nc group (Figures 4B–4D). Pre-treating HBV-infected cells with LAM (Nc + LAM) markedly reduced intracellular HBV DNA (Figure 4C) and, less prominently, secreted HBsAg levels (Figure 4B). HBV cccDNA amplification was blocked by LAM (Figures 4D and 4E) by day 17 post nucleofection, proving rcDNA → cccDNA conversion as the major mechanism supporting cccDNA *de novo* formation in HepG2-hNTCP cells. No significant reduction in HBV parameters observed at 7 days post nucleofection may be related to initially low HBV cccDNA levels formed in HepG2-hNTCP cells.

These data, acquired from an advanced HBV infection system, strengthen our major conclusion that HBV rcDNA → cccDNA is a crucial step supporting HBV persistence after HBV cccDNA was inactivated by CRISPR-Cas9. This strategy blocks amplification of HBV and results in gradual resolution of HBV infection. Nevertheless, it is important to understand whether these effects are reproduced in primary human hepatocytes and in patients *in vivo*.

DISCUSSION

The issue of virological cure of CHB is central in HBV research. Novel drugs and combinations can target virtually every step of HBV replication but still cannot completely cure CHB.[28] CRISPR-Cas9 systems very efficiently cleave target loci in HBV cccDNA, suppressing viral replication. However, most previous studies relied on continuous expression of CRISPR-Cas9 components to suppress HBV.[7,8,10,13,17,29] Continuous overexpression of gene-editing complexes is not a viable approach, as it dramatically raises the risks of off-target mutagenesis and toxicity.[30–32] Transient delivery of CRISPR-Cas9 systems in the form of RNPs is safer and provides rapid, burst-like editing of target sequences that could remove HBV cccDNA from infected cells and contribute to viral clearance.[19,33] Although we observed a prominent reduction in HBV cccDNA levels by CRISPR-Cas9 RNPs (Figure 1), they failed to eliminate HBV and

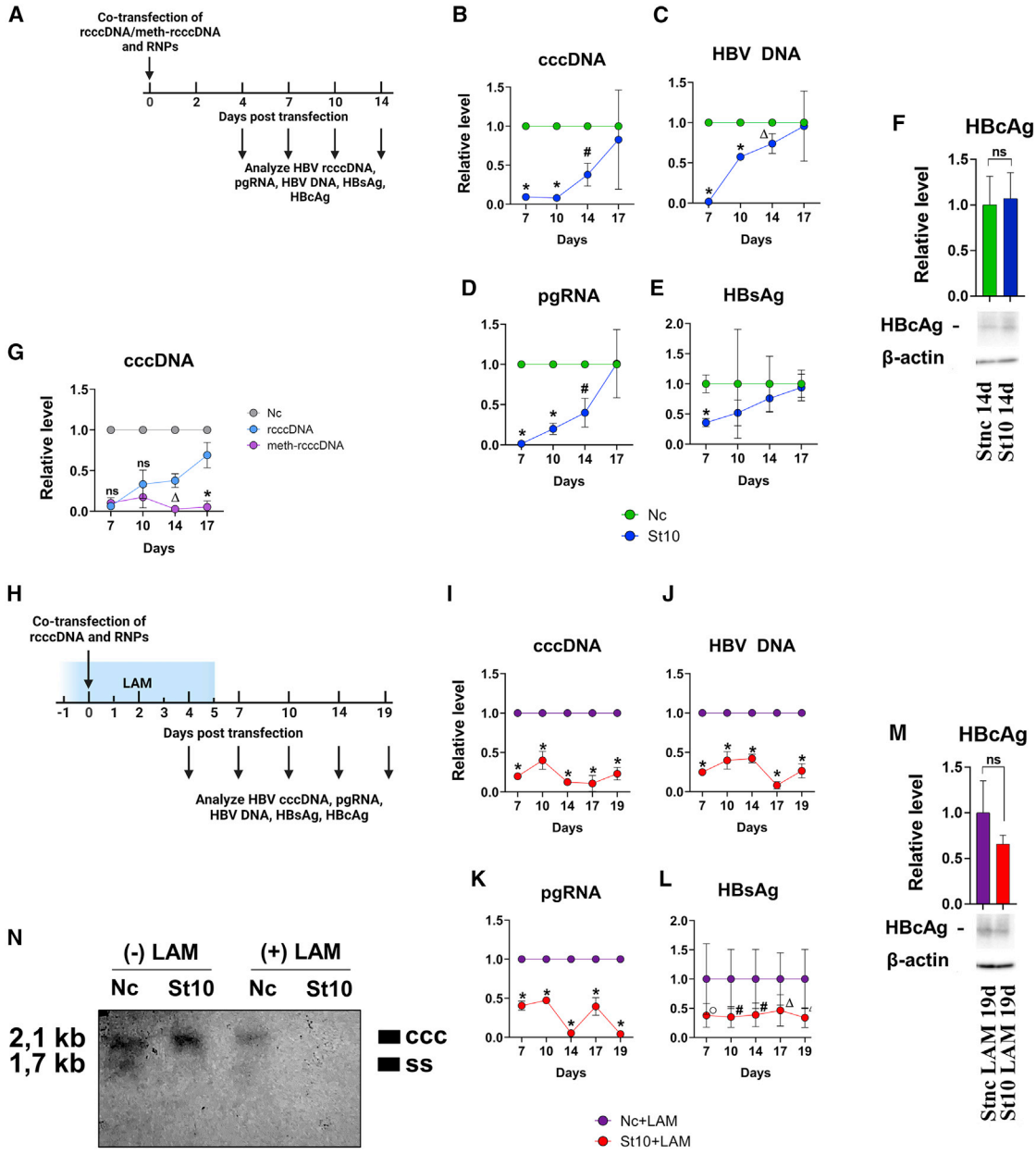

Figure 3. Rebound of HBV replication after CRISPR-Cas9 RNPs transfection and its prevention

(A) Experimental setup of a time-course experiment. (B–F) Changes in (B) HBV cccDNA, (C) intracellular HBV DNA, (D) pgRNA, (E) HBsAg, and (F) HBcAg levels (HBcAg dynamics is provided in Figure S7). (G) Dynamics of rcccDNA and meth-rcccDNA levels after StCas9/St10 RNPs transfection. (H) Experimental setup with LAM treatment. (I–M) Relative levels of HBV biomarkers compared with mock-treated controls. (N) Southern blot analysis of HBV intermediates at endpoints. HBV DNA and cccDNA levels are provided relative to β-globin; pgRNA levels are relative to GAPDH mRNA. $^{\circ}p < 0.05$, $^{\Delta}p < 0.01$, $^{\#}p < 0.001$, $^{*}p < 0.0001$; ns, not significant. (A) and (H) were created in BioRender.

were followed by reconstitution of HBV cccDNA and viral replication (Figures 3 and 4). HBV rcDNA, an intermediate able to recycle to the nucleus, was found to be the reason for viral rebound (Figure 4).

The important point is that even short-term LAM pre-treatment was sufficient to markedly improve anti-HBV activity of CRISPR-Cas9 RNPs and promote resolution of infection. The remaining (but declining) HBV intermediates (Figures 3 and 4) may be related to a small portion of cells which were not transfected/nucleofected or, potentially, to a small portion of HBV cccDNA which failed to be targeted by CRISPR-Cas9. Alternatively, new, deficient types of HBV cccDNA episomes may arise from activity of gene-editing complexes

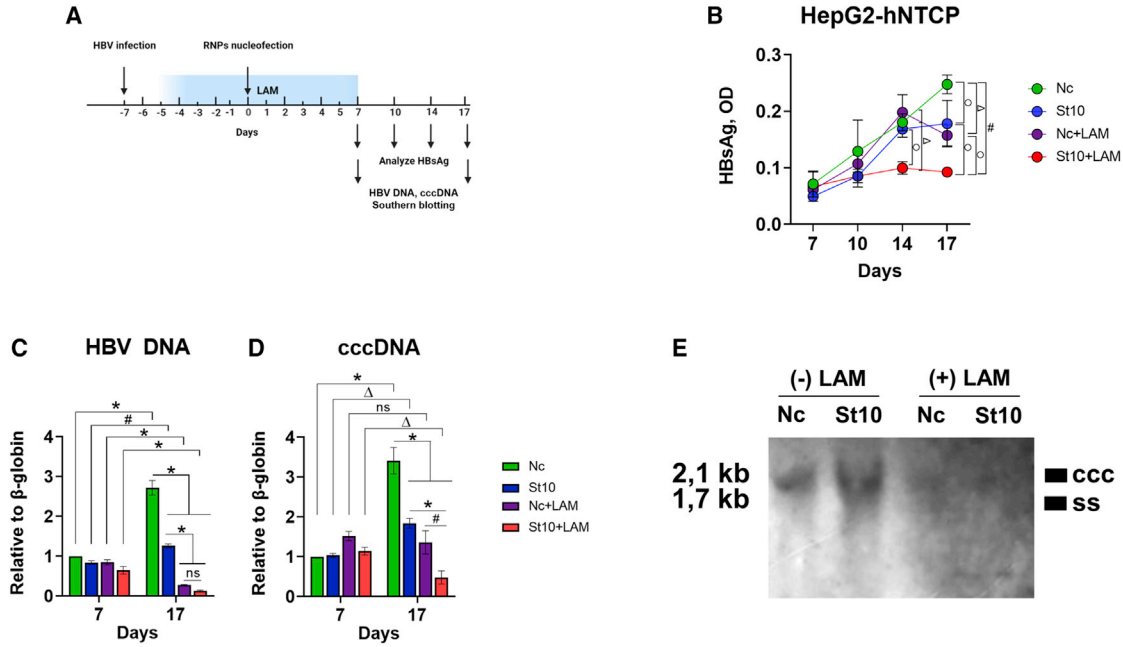

Figure 4. Effects of CRISPR-Cas9 RNPs and LAM at HepG2-NTCP infection model

(A) Experimental design. (B–D) Anti-HBV activity of CRISPR-Cas9 RNPs measured by (B) HBsAg, (C) HBV DNA, and (D) cccDNA. HBV DNA and cccDNA levels are provided relative to β-globin. (E) Southern blot analysis of HBV intermediates at an endpoint. Control rcccDNA was used in the same experiment as in Figure 3N. Nc, nucleofection of CRISPR-Cas9 RNPs with a non-targeting sgRNA; St10, nucleofection of CRISPR-Cas9 RNPs with HBV-targeting sgRNA St10. $^{\circ}p < 0.05$, $^{\Delta}p < 0.01$, $^{\#}p < 0.001$, $^{*}p < 0.0001$; ns, not significant. (A) was created in BioRender.

which appear to be produce transcriptionally silenced[7] or active[18] variants. Importantly, this study also explains previous observations that combination of CRISPR-Cas9 with reverse transcriptase inhibitors enhances their antiviral potency.[11,18] As shown in the HepG2-hNTCP infection model (Figure 4), rcDNA → cccDNA conversion appears to be the leading mechanism of *de novo* cccDNA synthesis. Our findings highlight the role of this step in HBV persistence, revealing it as an important barrier to a sterilizing cure of HBV infection and rcDNA as the important perpetrator of viral persistence. Understanding the role of HBV rcDNA → cccDNA conversion in persistence of HBV infection in other, non-transformed cell lines, such as primary human hepatocytes, as well as in CHB patients *in vivo*, is instrumental in developing "sterilizing" cure strategies.

RNA-interference (RNAi)-based anti-HBV therapies are rapidly advancing into the clinic, demonstrating potent antiviral activity by reducing all major viral RNA molecules.[34] Despite the promising results RNAi therapies are unlikely to become monotherapies, so revealing new, effective drug combinations is of critical importance.[35] RNAi therapies are currently studied in combination with traditional nucleot(s)ide analogs, peg-interferon-α, and viral entry inhibitors[36] to improve treatment outcomes and achieve a cure or stable post-treatment control of HBV replication. In light of our results, the use of RNAi therapies may have benefits compared with nucleot(s)ide analogs by effectively destabilizing pgRNA and countering HBV cccDNA *de novo* formation.

The fate of HBV cccDNA targeted by CRISPR-Cas9 is currently not clear. The pioneering studies observed both mutational inactivation[7,17,37] and degradation of HBV cccDNA.[11,13,20] Previously,[12] we identified that targeted HBV cccDNA (Figure 1D) is mostly destroyed by high-efficiency CRISPR-Cas9; the same effect of short-lived CRISPR-Cas9 RNPs was observed in this study, with >98% of targeted cccDNA undergoing degradation. In contrast, Martinez et al.[18] have recently argued that upon CRISPR-Cas targeting with two sgRNAs, HBV cccDNA is rather prone to the formation of new episomal, transcriptionally active cccDNA variants. The authors explain this discrepancy by non-physiological levels of HBV cccDNA in some *in vitro* systems used previously, which may be beyond the repair capacities of DNA repair pathways. However, HBV cccDNA was studied previously in infection systems.[7,8] Moreover, the overload of DNA repair systems is unlikely, as the capacity of DNA repair machinery is very high; hundreds of DSBs per cell are repaired when induced by irradiation, laser beams, or chemical treatment.[38] For understanding of the phenomenon of DNA degradation even upon a single nucleolytic cleavage, it is important to note the kinetics and repair of Cas9-induced DSBs. In contrast to physiological DSBs, DNA damage response factors are not recruited to Cas9-induced DSBs immediately because Cas9 stays tightly bound to one or both DNA ends. This results in slower and more erroneous repair and may lead to the loss of genomic sites, formation of large deletions or, when the target is small (as HBV cccDNA), may potentially lead to its decay by cellular nucleases. Another explanation could be that the dose, the type of

CRISPR-Cas9 system and target site, structure of damaged and local chromatin, and cell type per se could all potentially affect the outcomes of HBV cccDNA cleavage.[21,39–41] It is tempting to speculate that the fate HBV cccDNA cleavage could be controlled by different doses of gene-editing complexes.[42]

An intriguing feature of the HBV cccDNA pool is that it likely exists in many epigenetically distinct forms that can change in different phases of infection and during treatment.[24] Owing to reduced accessibility, gene editing in heterochromatin is diminished.[43,44] DNA methylation is not only associated with heterochromatin but can lower CRISPR-Cas9 activity per se.[26,27] We experimentally addressed whether the epigenetic state (DNA methylation) can impede antiviral properties of CRISPR-Cas9 RNPs and showed that it can severely reduce on-target nucleolytic activity. Even more importantly, this effect can be negated by increased RNP dosage (higher RNP-to-target ratio). Whether the presence of other epigenetic modifications or epigenetic profiles of HBV cccDNA interfere with CRISPR-Cas9 antiviral efficiency is unknown. According to our findings, DNA methylation blocks StCas9 nucleolytic and antiviral activity, but this effect can be resolved by using higher doses of RNPs.

Efficient systemic delivery of CRISPR-Cas9 RNPs is yet not possible, but many vehicles for packaging and tissue-specific delivery are under investigation.[45] We did not detect off-target activity of StCas9 either after continuous StCas9/sgRNA overexpression[13] or after transient RNP delivery (Figure S3). Nevertheless, the effects of different doses of CRISPR-Cas9 RNPs on off-target sites in the presence and, importantly, in the absence of target sequences must be determined. In uninfected cells, RNPs cannot occupy viral targets but instead may preferentially target host cell nucleic acids and induce undesirable mutagenesis. Although the question of off-target activity of CRISPR-Cas9 is apparently losing importance because of invention and discovery of high-fidelity Cas9 variants, for HBV therapy new molecular tools must be able to discriminate between episomal HBV cccDNA and integrated HBV genomes. Clearly, cleaving multiple HBV DNA integrations in infected cells can result in mutations, chromosome loss,[46] and eventual cell death, or, in the worst and very probable case, carcinogenesis.

Although less than a decade has elapsed since CRISPR-Cas9 was first used for gene editing in humans, these tools are now investigated in clinical trials as therapies for hereditary and infectious diseases and cancer. Our studies substantiate the utility of CRISPR-Cas9 RNPs for targeting HBV and provide the first strategy for resolution of HBV infection with a single dose of CRISPR-Cas9 RNPs.

MATERIALS AND METHODS

Cell culture and transfection

The human HepG2-1.1MerHBV, HepG2-1.5HBV (kindly provided by Dr. Dieter Glebe), and HepG2 cell lines were cultured in complete DMEM (high glucose) with 10% fetal bovine serum (FBS), 2 μM L-glutamine, and 1% penicillin/streptomycin. HepG2-1.1MerHBV was supplemented with 100 ng/μL doxycycline for 24 h to induce HBV replication, then doxycycline was removed, cells were washed twice with PBS, and fresh culture medium was added. HepG2 cells were transfected with rcccDNA or meth-rcccDNA and CRISPR-Cas9 RNP complexes using Lipofectamine CRISPRMAX transfection kit (Invitrogen). In brief, recombinant StCas9 protein was mixed with *in vitro*-transcribed sgRNA at 1:1 M ratio and rcccDNA/meth-rcccDNA in OptiMEM (Gibco) and incubated for 10 min. After 10 min, Cas9 Plus reagent was added to the StCas9/sgRNA complexes, mixed, and incubated for 10 min. In parallel, CRISPRMAX reagent was mixed with OptiMEM (Gibco) and was left for 10 min. Thereafter, CRISPRMAX mix was added to the Cas9/sgRNA complexes and incubated for another 10 min. The final mixture was added to the cells at 50% confluence.

Nucleofection

HepG2-hNTCP cells were transfected with StCas9/sgRNA pre-assembled complexes using LONZA Nucleofector according to the manufacturer's instructions with available HepG2-specific parameters. In brief, a total of 1 million cells were resuspended in SF Nucleofector solution and Supplement 1 containing pre-assembled StCas9 protein with sgRNA at a 1:1 M ratio. Cells were washed the next day post nucleofection and supplemented with complete medium.

Chemicals

Solution of NU7026 was added to cells at a final concentration of 7.5 μM in complete DMEM medium. NU7026-containing medium was changed every 1–2 days until harvest. DMSO was used as a mock-treatment control in experiments with NU7026. Lamivudine (LAM) was added to cells at a final concentration of 2 μM mixed with complete DMEM medium. Cells were incubated with LAM for 6 days, and fresh medium with LAM was added every 2 days. All chemicals were first added to cells 1 day before the transfection.

Synthesis of rcccDNA

rcccDNA was produced using minicircle technology as described previously.[47] In brief, HBV genome of genotype D sequence was cloned into minicircle producing plasmid containing attB and attP recombination sites (mini-HBV). Chemically competent *E. coli* strain ZYCY10P3S2T (System Biosciences) was transformed with the mini-HBV. Clones of successfully transformed cells were selected, and three colonies of *E. coli* were incubated in lysogeny broth (LB) with kanamycin at 37°C for 4 h. Next, 1 mL of the resulting cell suspension was inoculated to 200 mL of Terrific broth medium and incubated at 37°C overnight to an OD_{600} of 6–8 and pH of 7.0. Thereafter, it was mixed with 200 mL of induction medium (1 N NaOH and 0.2% L-arabinose in LB) and incubated first for 3 h at 30°C, then for 1 h at 37°C. rcccDNA was isolated from the resulting bacterial pellet using a Plasmid Maxi Kit (Qiagen, Germany).

Methylation of rcccDNA

HBV rcccDNA was methylated by M.SssI CpG methyltransferase (SibEnzyme) according to the manufacturer's protocol. In brief, 1 mg of rcccDNA was incubated with the M.SssI CpG

methyltransferase at 37°C for 30 min and then purified by a Qiagen PCR purification kit.

HBV infection of HepG2-hNTCP

HepG2-hNTPC cells were seeded onto collagen 1 (from rat tails) coated 6-well plates in high-glucose DMEM (Gibco) supplemented with 10% FBS (Biosera) at a density of 6×10^4 cells/well and grown to monolayer. After maintaining additional 3 days at monolayer without splitting, the medium was replaced with similar medium containing also 2% DMSO (Sigma). After an additional 72 h the cells were infected with HBV. In brief, HBV was added at a density of 650 genomic equivalents/cell in the presence of 4% polyethylene glycol 8000 (PEG-8000) in Williams E medium (Gibco) supplemented with GlutaMAX, 50 μM hydrocortisone, 5 μg/mL insulin, 2% FetalClone II (Thermo Fisher Scientific), 50 units/mL penicillin, and 50 μg/mL streptomycin. Twenty-four hours after infection the cells were washed with PBS (3 × 3 mL), and the fresh medium lacking PEG-8000 was added. Three days after infection, lamividin was added to the respective samples to a final concentration of 2 μM, and the medium was changed every 3 days.

HBV stock was obtained from HepG2.2.15 cells. These cells were seeded onto 20 10-cm Petri dishes coated with collagen 1 from rat tails at a density of 2×10^6 cells/dish in DMEM supplemented with 10% FBS (Biosera). Three days after the monolayer was formed, 2% DMSO was added for cell differentiation. After an additional 48 h the medium was replaced with DMEM-F12 medium (Gibco) containing 2.5% FetalClone II, and the conditioned medium was collected every 3 days during 2 weeks and stored at 4°C. Thereafter, the aliquots were combined, the virus was precipitated by addition of PEG-8000 to the final concentration of 4% with subsequent gentle shaking during 18 h, and centrifuged (3,000 × *g*, 1 h, 4°C). The supernatant was discarded, and the pellet was resuspended in 20 mL of Williams E medium with GlutaMAX, 50 μM hydrocortisone, 5 μg/mL insulin, 2% FetalClone II, and 50 units/mL penicillin/50 μg/mL streptomycin, aliquoted, and stored at −70°C.

Bisulfite sequencing

Unmethylated cytosines in the extracted DNA were converted to uracils using the EpiTect 96 Bisulfite Kit (Qiagen) according to the manufacturer's instructions. One microgram of DNA was subjected to a bisulfite conversion PCR protocol. PCR amplification of selected markers was performed using primers (Table S1) designed with the PyroMark Assay Design Software 1.0 (Qiagen). PCR reactions were carried out in a total volume of 25 μL, containing 0.2 μM of each of the primers, 20 ng of template DNA, and PCR Mix with TaqF polymerase, PCR buffer, and dNTPs (AmpliSens Biotechnologies). The amplification program consisted of an initial denaturation step at 95°C for 10 min, followed by five cycles comprising: denaturation (95°C for 45 s), annealing (60°C for 90 s), and extension (72°C for 2 min), followed by 25 cycles of denaturation (95°C for 45 s), annealing (60°C for 90 s), and extension (72°C for 90 s), and a final extension of 72°C for 10 min. Negative PCR controls were included in each PCR amplification. Pyrosequencing was performed using PyroMark Gold Q24 Reagents (Qiagen) with the PyroMark Q24 Vacuum Workstation and PyroMark Q24 instrument following the manufacturer's instructions. A 10-μL aliquot of the PCR product was immobilized to 2 μL of Streptavidin Sepharose High Performance (GE Healthcare). Annealing was carried out for 2 min at 80°C with 25 μL of 0.3 mM sequencing primer. The resulting Pyrogram traces were automatically analyzed using PyroMark analysis software v.2.0.8 (Qiagen).

In vitro transcription and purification of sgRNA

PCR product encoding appropriate sgRNA sequence under T7 promoter was synthesized using Q5 polymerase based on U6-PCR product as described previously,[12] with primers ultramerT7_f and ultramerSt1_r. Next, T7 containing PCR product was used as a template for *in vitro* transcription (IVT) reaction using the HiScribe Quick T7 High Yield RNA synthesis kit (NEB) according to the manufacturer's protocol. The IVT reaction was incubated overnight and then treated with DNAse I (NEB) for 15 min at 37°C followed by isopropanol purification. In brief, isopropanol and 0.5 M NaCl were added to the reaction mixture and centrifuged for 30 min. Next, the pellet was consecutively washed twice with 70% and 95% ethanol. The air-dried pellet was resuspended in RNase-free water and stored at −80°C. sgRNA spacer sequences and primers used for sgRNA synthesis are listed in Table S2.

Generation of recombinant Cas9 proteins

The protein was expressed in *E. coli* strain BL21 (DE3) pLysS cells (Novagen). Cells were grown in LB medium (supplemented with the appropriate antibiotic, 0.5% sucrose, 0.5% glycerol, 1 mM magnesium chloride, 50 mM Na_2HPO_4, 50 mM KH_2PO_4, and 25 mM $(NH_4)_2SO_4$) at 30°C to an OD_{600} of 1.2. Expression was induced by incubation for a further 16 h with 0.1 mM isopropyl β-D-1-thiogalactopyranoside at 18°C. The protein was purified by a combination of affinity and ion exchange chromatographic steps. Cells were resuspended in 50 mM Tris-HCl (pH 8.0), 500 mM NaCl, 1 mM PMSF, 0.2% Triton X-100, and 0.1% Tween 20, sonicated on ice, and centrifuged at 15,000 × *g* for 40 min. Clarified lysate was treated with 0.05% polyethyleneimine for 30 min at 4°C, the resulting suspension was centrifuged at 15,000 × *g* for 40 min, and the pellet was discarded. Supernatant was bound to Ni-chelating Sepharose (GE Healthcare). The resin was washed extensively with 50 mM Tris-HCl (pH 8.0), 500 mM NaCl, 0.05% and Igepal CA-630, and the bound protein was eluted in 50 mM Tris-HCl (pH 8.0), 150 mM NaCl, 0.3 M imidazole, and 10% glycerol. The protein was further bound to SP Sepharose (GE Healthcare) in 50 mM Tris-HCl (pH 7.5), 150 mM NaCl, 0.01% Triton X-100, and 2 mM DTT, eluting with a linear gradient of 150 mM to 1 M NaCl. The glycerol was added to 50% and protein stored at −20°C.

In vitro digestion reaction

Recombinant Cas9 was mixed with IVT sgRNA at a 1:1 M ratio in NEB3.1 buffer and incubated for 10 min to assemble ribonucleoprotein complexes, after which 300 ng of target rcccDNA/methrcccDNA was added to the mixture. The *in vitro* reaction was

incubated for 1 h at 37°C followed by an inactivation step at 98°C for 2 min. Results were visualized by gel electrophoresis using 0.8% gel.

Isolation of nucleic acids

Cell-culture medium was removed, then cells were washed twice with PBS and lysed in AmpliSens Riboprep lysis buffer (AmpliSens Biotechnologies). Nucleic acids were isolated using the AmpliSens Riboprep kit (AmpliSens Biotechnologies) according to the manufacturer's instructions. For RNA isolation, nucleic acids were treated with RNase-free DNase I (NEB) for 30 min at 37°C, purified by using an AmpliSens Riboprep kit (AmpliSens Biotechnologies), and reverse transcribed using AmpliSens Reverta-FL (AmpliSens Biotechnologies). HBV cccDNA was isolated via Hirt procedure as described previously,[48] followed by treatment with T5 exonuclease (NEB) at 37°C for 60 min and inactivation at 70°C for 20 min.

PCR analysis

Viral pgRNA and S-RNA expression levels were normalized to GAPDH mRNA as a reference. Total intracellular HBV DNA and cccDNA levels were normalized to genomic β-globin. All PCRs were performed with specific sets of primers and probes (Table S3). Relative expression levels were calculated via the ΔΔCt method.

Immunofluorescence

Cells seeded on glass coverslips were fixed in 4% paraformaldehyde for 10 min. Next, coverslips were washed three times in 50 mM Tris-HCl (pH 8.0), incubated for 30 min with blocking buffer (0.02% Triton X-100, 10% horse serum, and 150 mM NaCl in 50 mM Tris-HCl [pH 8.0]), and incubated with primary goat polyclonal anti-6XHis-tag antibodies to detect StCas9-6XHis-tag protein (ab9136, Abcam) and with mouse monoclonal anti-HBc antibodies (ab8637, Abcam) at room temperature for 1 h. The cells were washed three times for 5 min in washing buffer (0.02% Triton X-100 and 200 mM NaCl in 50 mM Tris-HCl [pH 8.0]), then incubated with secondary Alexa Fluor 647 donkey anti-goat immunoglobulin G (IgG) H&L (ab150131, Abcam) and Alexa Fluor 488 donkey anti-mouse IgG H&L antibodies (ab150105, Abcam). Alternatively, coverslips were stained only with primary mouse monoclonal anti-HBc antibodies (ab8637, Abcam) and secondary Alexa Fluor 594 goat anti-mouse IgG H&L antibodies (ab150116, Abcam). Cell nuclei were counterstained with Hoechst 33342 (1/10,000; ab228551, Abcam) at room temperature for 1 h. Coverslips were washed three times for 5 min in washing buffer and mounted with Fluoroshield reagent (Abcam). Images were captured using a Leica DMI6000 microscope with 100× immersion objectives. The research was done using equipment of the Core Centrum of Institute of Developmental Biology RAS.

Next-generation sequencing and analysis

On-target regions (Table S4) and potential off-target regions (Table S5) were amplified with pairs of specific primers using Q5 polymerase (NEB); amplicons were gel purified and extracted using a QIAquick Gel Extraction Kit (Qiagen), quantified with a Qubit 2.0 Fluorometer (Life Technologies), and pooled in equimolar ratios. Adapters for Illumina sequencing were then attached. Libraries were sequenced with paired-end 250 reads using MiSeq instrument (Illumina). FASTQC software and Geneious software were used for quality assessment, reference alignment, discarding low-quality reads and nucleotides, and calculating indels. Indels were calculated using custom Python scripts (available upon request).

HBsAg analysis

Cell-conditioned medium was harvested and filtered through 0.2-μm filters to remove cell debris. HBsAg quantification was performed using a colorimetric ELISA-based test system, DS-IFA-HBsAg-0,01 (Diagnostic Systems), according to the manufacturer's instructions (Diagnostic Systems, Nizhniy Novgorod, Russia).

Western blotting

Cells were harvested from 6-well plates at indicated time points, first lysed on ice with RIPA buffer for 10 min, then mixed with an equal volume of Laemmli buffer on ice and kept on ice for another 10 min. Thereafter, samples were denaturized by incubation at 95°C for 10 min. Samples were stored at −20°C until use. Proteins were resolved by 16% SDS-PAGE and transferred to a polyvinylidene fluoride membrane (Immobilon P, Sigma). Membranes were blocked with 5% fat-free powdered milk in PBST buffer (80 mM Na_2HPO_4, 20 mM NaH_2PO_4, 100 mM NaCl, 0.1% Tween 20) at room temperature for 1 h. Next, membranes were incubated with primary mouse anti-HBcAg (sc-23945, diluted at 1:5,000, Santa Cruz Biotechnology) monoclonal antibodies at 4°C overnight with gentle shaking, washed three times for 10 min with PBST, and incubated with secondary goat anti-mouse IgG (ab6789, diluted at 1:10,000, Abcam) antibodies conjugated with horseradish peroxidase. Finally, membranes were washed three times with PBST, and signal was developed using ECL reagent (Thermo Fisher) and detected with X-ray films or G-box. Membranes were then stripped using mild stripping buffer (1.5% glycine, 0.1% SDS, 1% Tween 20 [pH 2.2]) and restained with primary mouse anti-β-actin (A5441, 1:10,000, Sigma) monoclonal antibodies for 1 h at room temperature, washed three times with PBST, and incubated with secondary goat anti-mouse IgG (ab6789, 1:10,000, Abcam) antibodies conjugated with horseradish peroxidase. Results were analyzed using ImageJ software.

Southern blotting

HBV cccDNA was isolated from cells using a RiboPrep kit (Amplisense Biosciences) and detected by Southern blotting as described previously[48] with modifications. In brief, DNA isolates were heated at 85°C for 5 min, run on 1.2% agarose gel electrophoresis, and blotted onto a HybondTM-N+ membrane (GE Healthcare). Biotin labeling of a mixture of HBV-specific DNA probes was performed using a North2South Biotin Random Prime DNA Labeling kit (Thermo Fisher). After pre-hybridization at 55°C for 30 min in North2South Chemiluminescent Detection kit hybridization buffer (Thermo Fisher), 30 ng/mL labeled probes was hybridized at 55°C for 48 h in hybridization buffer. DNA probe-cccDNA hybrids were visualized using Streptavidin:HRP conjugates with SuperSignal West Femto Maximum Sensitivity Substrate (Thermo Fisher) peroxide/luminol solution.

Statistical analysis

Values were expressed as mean ± SD of triplicate experiments in GraphPad Prism software. Student's t test with Tukey's HSD post hoc test was used to compare variables and calculate p values to identify statistically significant differences in means. To determine whether each off-target indel rate in deep-sequencing analysis is significant compared with mock-treated control samples, a two-tailed p value was calculated using Fisher's exact test.

DATA AVAILABILITY

Python codes are available upon reasonable request.

SUPPLEMENTAL INFORMATION

Supplemental information can be found online at https://doi.org/10.1016/j.omtn.2023.02.001.

ACKNOWLEDGMENTS

This study was funded by RSF grant no. 20-15-00373 with the exception of experiments with HepG2-hNTPC cells, which were supported by the Russian Ministry of Science and Higher Education of the Russian Federation (agreement 075-15-2019-1660). We thank Prof. Dieter Glebe for valuable discussions.

AUTHOR CONTRIBUTIONS

D.K. was responsible for the study concept, funding acquisition and, together with A.K. and S.B., for study design, conducting of all experiments, analysis, data interpretation, and drafting and revisions of the manuscript. N.P. participated in all experiments, acquired and analyzed PCR data. N.F.Z. and D.V.Y. performed experiments with HepG2-hNTCP cells. V.C. obtained funding, supervised the study, and revised the manuscript. I. Goptar, A.N., and A.S. generated and purified StCas9 proteins. E.D. performed bisulfite sequencing. E.B. acquired western blot results and revised the manuscript. T.L. and I.A. conducted deep sequencing. A.F., A.E., S.B., N.P., A.K., D.K. and A.A.Z. performed Southern blotting. A.I. assisted in LAM experiments and revised the manuscript. I. Gordeychuk and A.L. revised the manuscript.

DECLARATION OF INTERESTS

The authors declare no competing interests.

REFERENCES

1. Glebe, D., and Bremer, C. (2013). The molecular virology of hepatitis B virus. Semin. Liver Dis. *33*, 103–112. https://doi.org/10.1055/s-0033-1345717.
2. World Health Organization. Global Hepatitis Report, 2017; 2017. ISBN 978-92-4-156545-5.
3. Chen, C.-H., Lu, S.-N., Hung, C.-H., Wang, J.-H., Hu, T.-H., Changchien, C.-S., and Lee, C.-M. (2014). The role of hepatitis B surface antigen quantification in predicting HBsAg loss and HBV relapse after discontinuation of lamivudine treatment. J. Hepatol. *61*, 515–522.
4. Werle–Lapostolle, B., Bowden, S., Locarnini, S., Wursthorn, K., Petersen, J., Lau, G., Trepo, C., Marcellin, P., Goodman, Z., Delaney, W.E., 4th, et al. (2004). Persistence of cccDNA during the natural history of chronic hepatitis B and decline during adefovir dipivoxil therapy. Gastroenterology *126*, 1750–1758.
5. Revill, P.A., Chisari, F.V., Block, J.M., Dandri, M., Gehring, A.J., Guo, H., Hu, J., Kramvis, A., Lampertico, P., Janssen, H.L.A., et al. (2019). A global scientific strategy to cure hepatitis B. Lancet Gastroenterol. Hepatol. *4*, 545–558. https://doi.org/10.1016/S2468-1253(19)30119-0.
6. Mali, P., Yang, L., Esvelt, K.M., Aach, J., Guell, M., DiCarlo, J.E., Norville, J.E., and Church, G.M. (2013). RNA-guided human genome engineering via Cas9. Science *339*, 823–826.
7. Seeger, C., and Sohn, J.A. (2016). Complete spectrum of CRISPR/Cas9-induced mutations on HBV cccDNA. Mol. Ther. *24*, 1258–1266. https://doi.org/10.1038/mt.2016.94.
8. Seeger, C., and Sohn, J.A. (2014). Targeting hepatitis B virus with CRISPR/Cas9. Mol. Ther. Nucleic Acids *3*, e216. https://doi.org/10.1038/mtna.2014.68.
9. Lin, S.-R.R., Yang, H.-C.C., Kuo, Y.-T.T., Liu, C.-J., Yang, T.-Y., Sung, K.-C., Lin, Y.-Y., Wang, H.-Y., Wang, C.-C., Shen, Y.-C., et al. (2014). The CRISPR/Cas9 system facilitates clearance of the intrahepatic HBV templates in vivo. Mol. Ther. Nucleic Acids *3*, e186. https://doi.org/10.1038/mtna.2014.38.
10. Zhu, W., Xie, K., Xu, Y., Wang, L., Chen, K., Zhang, L., and Fang, J. (2016). CRISPR/Cas9 produces anti-hepatitis B virus effect in hepatoma cells and transgenic mouse. Virus Res. *217*, 125–132. https://doi.org/10.1016/j.virusres.2016.04.003.
11. Kennedy, E.M., Bassit, L.C., Mueller, H., Kornepati, A.V.R., Bogerd, H.P., Nie, T., Chatterjee, P., Javanbakht, H., Schinazi, R.F., and Cullen, B.R. (2015). Suppression of hepatitis B virus DNA accumulation in chronically infected cells using a bacterial CRISPR/Cas RNA-guided DNA endonuclease. Virology *476*, 196–205. https://doi.org/10.1016/j.virol.2014.12.001.
12. Kostyushev, D., Kostyusheva, A., Brezgin, S., Zarifyan, D., Utkina, A., Goptar, I., and Chulanov, V. (2019). Suppressing the NHEJ pathway by DNA-PKcs inhibitor NU7026 prevents degradation of HBV cccDNA cleaved by CRISPR/Cas9. Sci. Rep. *9*, 1847.
13. Kostyushev, D., Brezgin, S., Kostyusheva, A., Zarifyan, D., Goptar, I., and Chulanov, V. (2019). Orthologous CRISPR/Cas9 systems for specific and efficient degradation of covalently closed circular DNA of hepatitis B virus. Cell. Mol. Life Sci. *76*, 1779–1794. https://doi.org/10.1007/s00018-019-03021-8.
14. Ko, C., Chakraborty, A., Chou, W.-M., Hasreiter, J., Wettengel, J.M., Stadler, D., Bester, R., Asen, T., Zhang, K., Wisskirchen, K., et al. (2018). Hepatitis B virus (HBV) genome recycling and de novo secondary infection events maintain stable cccDNA levels. J. Hepatol. *69*, 1231–1241.
15. Wang, J., Xu, Z.W., Liu, S., Zhang, R.-Y., Ding, S.-L., Xie, X.-M., Long, L., Chen, X.-M., Zhuang, H., and Lu, F.-M. (2015). Dual gRNAs guided CRISPR/Cas9 system inhibits hepatitis B virus replication. World J. Gastroenterol. *21*, 9554–9565. https://doi.org/10.3748/wjg.v21.i32.9554.
16. Ramanan, V., Shlomai, A., Cox, D.B.T., Schwartz, R.E., Michailidis, E., Bhatta, A., Scott, D.A., Zhang, F., Rice, C.M., and Bhatia, S.N. (2015). CRISPR/Cas9 cleavage of viral DNA efficiently suppresses hepatitis B virus. Sci. Rep. *5*, 10833. https://doi.org/10.1038/srep10833.
17. Liu, X., Hao, R., Chen, S., Guo, D., and Chen, Y. (2015). Inhibition of hepatitis B virus by the CRISPR/Cas9 system via targeting the conserved regions of the viral genome. J. Gen. Virol. *96*, 2252–2261.
18. Martinez, M.G., Combe, E., Inchauspe, A., Mangeot, P.E., Delberghe, E., Chapus, F., Neveu, G., Alam, A., Carter, K., Testoni, B., et al. (2022). CRISPR-Cas9 targeting of hepatitis B virus covalently closed circular DNA generates transcriptionally active episomal variants. mBio *13*, e0288821. https://doi.org/10.1128/mbio.02888-21.
19. Kim, K., Park, S.W., Kim, J.H., Lee, S.H., Kim, D., Koo, T., Kim, K.-E., Kim, J.H., and Kim, J.-S. (2017). Genome surgery using Cas9 ribonucleoproteins for the treatment of age-related macular degeneration. Genome Res. *27*, 419–426. https://doi.org/10.1101/gr.219089.116.
20. Liu, Y., Zhao, M., Gong, M., Xu, Y., Xie, C., Deng, H., Li, X., Wu, H., and Wang, Z. (2018). Inhibition of hepatitis B virus replication via HBV DNA cleavage by Cas9 from Staphylococcus aureus. Antivir. Res. *152*, 58–67. https://doi.org/10.1016/j.antiviral.2018.02.011.
21. Brinkman, E.K., Chen, T., de Haas, M., Holland, H.A., Akhtar, W., and van Steensel, B. (2018). Kinetics and fidelity of the repair of Cas9-induced double-strand DNA breaks. Mol. Cell *70*, 801–813.e6. https://doi.org/10.1016/j.molcel.2018.04.016.
22. Kostyushev, D., Kostyusheva, A., Ponomareva, N., Brezgin, S., and Chulanov, V. (2022). CRISPR/Cas and hepatitis B therapy: technological advances and practical barriers. Nucleic Acid Therapeut. *32*, 14–28. https://doi.org/10.1089/nat.2021.0075.

23. Jain, S., Chang, T.-T., Chen, S., Boldbaatar, B., Clemens, A., Lin, S.Y., Yan, R., Hu, C.-T., Guo, H., Block, T.M., et al. (2015). Comprehensive DNA methylation analysis of hepatitis B virus genome in infected liver tissues. Sci. Rep. *5*, 10478. https://doi.org/10.1038/srep10478.

24. Tropberger, P., Mercier, A., Robinson, M., Zhong, W., Ganem, D.E., and Holdorf, M. (2015). Mapping of histone modifications in episomal HBV cccDNA uncovers an unusual chromatin organization amenable to epigenetic manipulation. Proc. Natl. Acad. Sci. USA *112*, E5715–E5724. https://doi.org/10.1073/pnas.1518090112.

25. Lucifora, J., Xia, Y., Reisinger, F., Zhang, K., Stadler, D., Cheng, X., Sprinzl, M.F., Koppensteiner, H., Makowska, Z., Volz, T., et al. (2014). Specific and nonhepatotoxic degradation of nuclear hepatitis B virus cccDNA. Science *343*, 1221–1228. https://doi.org/10.1126/science.1243462.

26. Das, A., Hand, T.H., Smith, C.L., Wickline, E., Zawrotny, M., and Li, H. (2020). The molecular basis for recognition of 5′-NNNCC-3′ PAM and its methylation state by Acidothermus cellulolyticus Cas9. Nat. Commun. *11*, 1–11.

27. Liu, Y., Li, J., Zhou, C., Meng, B., Wei, Y., Yang, G., Lu, Z., Shen, Q., Zhang, Y., Yang, H., et al. (2019). Allele-specific genome editing of imprinting genes by preferentially targeting non-methylated loci using Staphylococcus aureus Cas9 (SaCas9). Sci. Bull. *64*, 1592–1600.

28. Yang, S., Zeng, W., Zhang, J., Lu, F., Chang, J., and Guo, J.-T. (2021). Restoration of a functional antiviral immune response to chronic HBV infection by reducing viral antigen load: if not sufficient, is it necessary? Emerg. Microb. Infect. *10*, 1545–1554. https://doi.org/10.1080/22221751.2021.1952851.

29. Lin, S.R., Yang, H.C., Kuo, Y.T., Liu, C.-J., Yang, T.-Y., Sung, K.-C., Lin, Y.-Y., Wang, H.-Y., Wang, C.-C., Shen, Y.-C., et al. (2014). The CRISPR/Cas9 system facilitates clearance of the intrahepatic HBV templates in vivo. Mol. Ther. Nucleic Acids *3*, e186. https://doi.org/10.1038/mtna.2014.38.

30. Zhang, X.H., Tee, L.Y., Wang, X.G., Huang, Q.S., and Yang, S.H. (2015). Off-target effects in CRISPR/Cas9-mediated genome engineering. Mol. Ther. Nucleic Acids *4*. https://doi.org/10.1038/mtna.2015.37.

31. Wang, L., Shao, Y., Guan, Y., Li, L., Wu, L., Chen, F., Liu, M., Chen, H., Ma, Y., Ma, X., et al. (2015). Large genomic fragment deletion and functional gene cassette knock-in via Cas9 protein mediated genome editing in one-cell rodent embryos. Sci. Rep. *5*, 17517. https://doi.org/10.1038/srep17517.

32. Li, A., Tanner, M.R., Lee, C.M., Hurley, A.E., Giorgi, M.D., Jarrett, K.E., Davis, T.H., Doerfler, A.M., Bao, G., Beeton, C., et al. (2020). AAV-CRISPR gene editing is negated by pre-existing immunity to Cas9. Mol. Ther. *28*, 1432–1441.

33. Kim, S., Kim, D., Cho, S.W., Kim, J., and Kim, J.-S. (2014). Highly efficient RNA-guided genome editing in human cells via delivery of purified Cas9 ribonucleoproteins. Genome Res. *24*, 1012–1019. https://doi.org/10.1101/gr.171322.113.

34. Yuen, M., Schiefke, I., Yoon, J., Ahn, S.H., Heo, J., Kim, J.H., Chan, H.L.Y., Yoon, K.T., Klinker, H., Manns, M., et al. (2020). RNA interference therapy with ARC-520 results in prolonged hepatitis B surface antigen response in patients with chronic hepatitis B infection. Hepatology *72*, 19–31.

35. Nayagam, J.S., Cargill, Z.C., and Agarwal, K. (2020). The role of RNA interference in functional cure strategies for chronic hepatitis B. Curr. Hepatol. Rep. *19*, 362–369.

36. Allweiss, L., Giersch, K., Pirosu, A., Volz, T., Muench, R.C., Beran, R.K., Urban, S., Javanbakht, H., Fletcher, S.P., Lütgehetmann, M., et al. (2022). Therapeutic shutdown of HBV transcripts promotes reappearance of the SMC5/6 complex and silencing of the viral genome in vivo. Gut *71*, 372–381.

37. Zhen, S., Hua, L., Liu, Y., Gao, L.-C., Fu, J., Wan, D.-Y., Dong, L.-H., Song, H.-F., and Gao, X. (2015). Harnessing the clustered regularly interspaced short palindromic repeat (CRISPR)/CRISPR-associated Cas9 system to disrupt the hepatitis B virus. Gene Ther. *22*, 404–412. https://doi.org/10.1038/gt.2015.2.

38. Wang, Y., Niu, J., Liu, J., and Sun, Y. (2022). Digital counting of breaks labeling in situ: a fast and absolute quantification method for measurement of DNA double-strand breaks based on digital polymerase chain reaction. Anal. Chem. *94*, 16871–16876.

39. Bothmer, A., Phadke, T., Barrera, L.A., Margulies, C.M., Lee, C.S., Buquicchio, F., Moss, S., Abdulkerim, H.S., Selleck, W., Jayaram, H., et al. (2017). Characterization of the interplay between DNA repair and CRISPR/Cas9-induced DNA lesions at an endogenous locus. Nat. Commun. *8*, 13905. https://doi.org/10.1038/ncomms13905.

40. Vriend, L.E.M., Prakash, R., Chen, C.-C., Vanoli, F., Cavallo, F., Zhang, Y., Jasin, M., and Krawczyk, P.M. (2016). Distinct genetic control of homologous recombination repair of Cas9-induced double-strand breaks, nicks and paired nicks. Nucleic Acids Res. *44*, 5204–5217.

41. Schep, R., Brinkman, E.K., Leemans, C., Vergara, X., van der Weide, R.H., Morris, B., van Schaik, T., Manzo, S.G., Peric-Hupkes, D., van den Berg, J., et al. (2021). Impact of chromatin context on Cas9-induced DNA double-strand break repair pathway balance. Mol. Cell *81*, 2216–2230.

42. Kostyushev, D., Kostyusheva, A., Ponomareva, N., Brezgin, S., and Chulanov, V. (2021). CRISPR/Cas and hepatitis B therapy: technological advances and practical barriers. Nucleic Acid Therapeut. *32*, 14–28.

43. Jain, S., Shukla, S., Yang, C., Zhang, M., Fatma, Z., Lingamaneni, M., Abesteh, S., Lane, S.T., Xiong, X., Wang, Y., et al. (2021). TALEN outperforms Cas9 in editing heterochromatin target sites. Nat. Commun. *12*, 1–10.

44. Kallimasioti-Pazi, E.M., Thelakkad Chathoth, K., Taylor, G.C., Meynert, A., Ballinger, T., Kelder, M.J.E., Lalevee, S., Sanli, I., Feil, R., and Wood, A.J. (2018). Heterochromatin delays CRISPR-Cas9 mutagenesis but does not influence the outcome of mutagenic DNA repair. PLoS Biol. *16*, e2005595.

45. Kostyushev, D., Kostyusheva, A., Brezgin, S., Smirnov, V., Volchkova, E., Lukashev, A., and Chulanov, V. (2020). Gene editing by extracellular vesicles. Int. J. Mol. Sci. *21*, 7362.

46. Cullot, G., Boutin, J., Toutain, J., Prat, F., Pennamen, P., Rooryck, C., Teichmann, M., Rousseau, E., Lamrissi-Garcia, I., Guyonnet-Duperat, V., et al. (2019). CRISPR-Cas9 genome editing induces megabase-scale chromosomal truncations. Nat. Commun. *10*, 1–14.

47. Guo, X., Chen, P., Hou, X., Xu, W., Wang, D., Wang, T.-Y., Zhang, L., Zheng, G., Gao, Z.-L., He, C.-Y., et al. (2016). The recombined cccDNA produced using minicircle technology mimicked HBV genome in structure and function closely. Sci. Rep. *6*, 25552. https://doi.org/10.1038/srep25552.

48. Cai, D., Nie, H., Yan, R., Guo, J.-T., Block, T.M., and Guo, H. (2013). A southern blot assay for detection of hepatitis B virus covalently closed circular DNA from cell cultures. Methods Mol. Biol. *1030*, 151–161. https://doi.org/10.1007/978-1-62703-484-5_13.